

Role of interaction in the binding of two Spin-orbit Coupled Fermions

Chong Ye,^{1,2} Jie Liu,^{2,3} Li-Bin Fu^{1,*}

¹Graduate School, China Academy of Engineering Physics, Beijing 100193, China

²National Laboratory of Science and Technology on Computational Physics,

³Institute of Applied Physics and Computational Mathematics, Beijing 100088, China

³HEDPS, CAPT, and CICIFSA MoE, Peking University, Beijing 100871, China

We investigate role of an attractive s-wave interaction with positive scattering length in the binding of two spin-orbit coupled fermions in the vacuum and on the top of a Fermi sea in the single impurity system, motivated by current interests in exploring exotic binding properties in the appearance of spin-orbit couplings. For weak spin-orbit couplings where the density of states is not significantly altered, we analytically show that the high-energy states become more important in determining the binding energy when the scattering length decreases. Consequently, tuning the interaction gives rise to a rich behavior, including a zigzag of the momentum of the bound state or inducing transitions among the meta-stable states. By exactly solving the two-body quantum mechanics for a spin-orbit coupled Fermi mixture of ^{40}K - ^{40}K - ^6Li , we demonstrate that our analysis can also apply to the case when the density of states is significantly modified by the spin-orbit coupling. Our findings pave a way for understanding and controlling the binding of fermions in the presence of spin orbit couplings.

PACS numbers: 03.65.Ge, 71.70.Ej, 67.85.Lm

I. INTRODUCTION

In ultracold physics, many schemes have been proposed to generate various types of synthetic spin-orbit couplings (SOC) by controlling atom-light interaction [1]. In 2011, I. B. Spielman's group in NIST had generated an equal weight combination of Rashba-type and Dresselhaus-type SOC in ^{87}Rb [2]. Afterwards, SOC has triggered a great amount of experimental interest [3–5]. In the appearance of SOC, the ultracold atomic gases have been altered dramatically [6–8].

One basic issue is the binding of two spin-orbit coupled fermions in the vacuum [9–16] where SOC has given rise to the change of binding energy and the appearance of finite-momentum dimer bound states. Another relevant issue is the binding of two fermions on the top of a Fermi sea (the molecular state) for the case where a single impurity is immersed in a noninteracting Fermi gas [16–21]. In the appearance of SOC, the center-of-mass (c.m.) momentum of the molecular state becomes finite [16, 21]. All of these can be understood from the perspective of two-body quantum mechanics. It generally contains three components: the threshold energy associated with the c.m. momentum, the density of states, and the interacting strength. For extremely weak attractive interaction, changes of two-body properties under SOC came from the different threshold behavior of the density of states [9, 10, 14]. However, in the strong interacting regime, the binding of two fermions presents a rich behavior [13, 16] such as the variation of the c.m. momentum and the competition between two meta-stable states with the tuning of interacting strength. These phenomena can

not simply owe to the threshold behavior of the density of states. Therefore, the mechanism as to how all these three components cooperate with each other in determining the novel two-body properties is pressing needed. The establishment of such a comprehensive picture will shed light on ongoing explorations of the intriguing behavior of spin-orbit coupled Fermi gases [9–16]. Below, we report a theoretical contribution to address this issue, which also allows predictions of new phenomena.

We investigate the two-body quantum mechanisms of the binding of two spin-orbit coupled fermions in the vacuum and on the top of a Fermi sea in the single impurity Fermi gas. We consider an attractive s-wave interaction with positive scattering length, the strength of which can be tuned in a wide range via a Feshbach resonance [22]. From Sec. II to Sec. IV, we give analyses which do not depend on the concrete type of SOC. In Sec. II, by decomposing the two-body energy (molecular energy) into the threshold energy and the binding energy, both of which depend on the c.m. momentum of two fermions, we establish a direct relation between the interaction, the density of states, and the binding energy. In Sec. III, with the first-order perturbation analysis in the weak SOC limit, we reveal that the low-energy states play a decisive role in determining the binding energy when the scattering length is large, in contrast to the small scattering length case where the high-energy states can dominate. This allows us to elucidate the mechanism underlying interesting phenomena such as a zigzag behavior of the two-body ground state momentum and the competition between two meta-stable states in Sec. IV. In Sec. V, we illustrate our analysis with an interacting Fermi mixture of ^{40}K - ^{40}K - ^6Li with ^{40}K containing an $(\alpha k_x \sigma_z + h \sigma_x)$ -type SOC, which can be realized by the state-of-the-art experimental techniques using cold atoms [4, 23]. Remarkably, by exactly solving the two-

* lbfu@gscaep.ac.cn

body problem for this system, we show that our analysis affords insights into the main properties of the binding of two spin-orbit coupled fermions, even when the density of states is significantly altered by SOC. Our findings reveal the role of interaction in the binding of two spin-orbit coupled fermions and allow deep physical understandings of the rich two-body properties in the presence of SOC.

II. BINDING OF TWO FERMIONS WITH SOC

We consider two different spin-orbit coupled fermionic species in three dimensions (3D) at zero temperature: atom A (B) has N_a (N_b) components, with the corresponding non-interacting Hamiltonian H_a (H_b). We consider an attractive s-wave contact interaction with positive scattering length between the two fermionic species as described by

$$H_{int} = \frac{U}{V} \sum_{\mathbf{Q}, \mathbf{k}, \mathbf{k}'} a_{\mathbf{k}, l_0}^\dagger b_{\mathbf{Q}-\mathbf{k}, m_0}^\dagger a_{\mathbf{k}', l_0} b_{\mathbf{Q}-\mathbf{k}', m_0}, \quad (1)$$

with \mathbf{Q} the c.m. momentum of two scattering fermions. Here $a_{\mathbf{k}, l_0}^\dagger$ ($b_{\mathbf{k}, m_0}^\dagger$) denotes the creation operator of a SOC-free atom A (B) in the l_0 -th (m_0 -th) spin component with momentum \mathbf{k} , U is the bare interaction, and V is the quantization volume. The total Hamiltonian is thus $H = H_a + H_b + H_{int}$.

With this Hamiltonian, we address to the binding of two fermionic atoms A and B (i) in the vacuum [9–16] and (ii) on the top of a non-interacting Fermi sea of atoms A in the situation where a single impurity of B is immersed in a non-interacting Fermi gas of A [17–21]. The ansatz wave function of the two-body bound state and the molecular state can be expressed in a general form

$$|\Psi_{\mathbf{Q}}\rangle = \sum_{i,j} \sum_{\mathbf{k}} \psi_{\mathbf{Q}, \mathbf{k}}^{i,j} \alpha_{\mathbf{k}, i}^\dagger \beta_{\mathbf{Q}-\mathbf{k}, j}^\dagger |\emptyset\rangle, \quad (2)$$

where \mathbf{Q} is the c.m. momentum of two particles. For (i), $|\emptyset\rangle$ is the vacuum state and the summation $\sum_{\mathbf{k}}$ includes all the states. For (ii), $|\emptyset\rangle$ is the non-interacting spin-orbit coupled Fermi sea of A and the summation $\sum_{\mathbf{k}}$ excludes the states below the Fermi surfaces, reflecting the effect of Pauli blocking. Here, $\alpha_{\mathbf{k}, i}^\dagger = \sum_{i'} \lambda_{\mathbf{k}}^{i, i'} a_{\mathbf{k}, i'}^\dagger$ ($\beta_{\mathbf{k}, i}^\dagger = \sum_{i'} \eta_{\mathbf{k}}^{i, i'} b_{\mathbf{k}, i'}^\dagger$) is the creation operator of an atom A (B) in the i -th eigen-state of Hamiltonian H_a (H_b) with momentum \mathbf{k} and energy $\varepsilon_{\mathbf{k}, i}^a$ ($\varepsilon_{\mathbf{k}, i}^b$) and $\psi_{\mathbf{Q}, \mathbf{k}}^{i,j}$ denotes the variational coefficient. The coefficients $\lambda_{\mathbf{k}}^{i, i'}$ and $\eta_{\mathbf{k}}^{i, i'}$ are fixed by SOC. Solving the eigen-equation $H|\Psi_{\mathbf{Q}}\rangle = E_{\mathbf{Q}}|\Psi_{\mathbf{Q}}\rangle$ gives

$$\psi_{\mathbf{Q}, \mathbf{k}}^{i,j} = \frac{(\lambda_{\mathbf{k}}^{i, l_0} \eta_{\mathbf{Q}-\mathbf{k}}^{j, m_0})^* U}{E_{\mathbf{Q}} - E_{\mathbf{Q}, \mathbf{k}}^{ij}} \frac{1}{V} \sum_{\mathbf{k}', i', j'} \psi_{\mathbf{Q}, \mathbf{k}'}^{i', j'} \lambda_{\mathbf{k}'}^{i', l_0} \eta_{\mathbf{Q}-\mathbf{k}'}^{j', m_0}, \quad (3)$$

with $E_{\mathbf{Q}, \mathbf{k}}^{ij} = \varepsilon_{\mathbf{k}, i}^a + \varepsilon_{\mathbf{Q}-\mathbf{k}, j}^b$. Rearranging Eq. (3), we obtain a self-consistent equation for two-body energy

(molecular energy) $E_{\mathbf{Q}}$ in the momentum-space representation, i.e.,

$$\frac{1}{U} = \frac{1}{V} \sum_{i,j} \sum_{\mathbf{k}} \frac{|\lambda_{\mathbf{k}}^{i, l_0}|^2 |\eta_{\mathbf{Q}-\mathbf{k}}^{j, m_0}|^2}{E_{\mathbf{Q}} - E_{\mathbf{Q}, \mathbf{k}}^{ij}}. \quad (4)$$

A key step of our treatment next constitutes a decomposition of $E_{\mathbf{Q}}$: Defining the threshold energy associated with the c.m. momentum \mathbf{Q} by $E_{th}^{\mathbf{Q}} \equiv \min_{i,j,\mathbf{k}} \{E_{\mathbf{Q}, \mathbf{k}}^{ij}\}$, we write $E_{\mathbf{Q}}^{ij} = E_{th}^{\mathbf{Q}} + \varepsilon$. The rest of the two-body energy (molecular energy) is therefore $E_{\mathbf{Q}}^{sc} \equiv E_{\mathbf{Q}} - E_{th}^{\mathbf{Q}}$. While $E_{th}^{\mathbf{Q}}$ is only affected by SOC, $E_{\mathbf{Q}}^{sc}$ encodes the effect of interaction. Such decomposition of $E_{\mathbf{Q}}$ in terms of $E_{\mathbf{Q}}^{sc}$ and $E_{th}^{\mathbf{Q}}$, as we shall see, allows a transparent correspondence to the SOC-free counterpart. Following a standard procedure, we obtain the self-consistent equation for $E_{\mathbf{Q}}^{sc}$ in the energy domain of ε as in Ref.[24]

$$\int_0^\infty \frac{\gamma_{\mathbf{Q}}^\varepsilon d\varepsilon}{E_{\mathbf{Q}}^{sc} - \varepsilon} = \frac{1}{U}. \quad (5)$$

Here, $\gamma_{\mathbf{Q}}^\varepsilon$ is defined by

$$\gamma_{\mathbf{Q}}^\varepsilon = \sum_i \sum_j \int' |\lambda_{\mathbf{k}}^{i, l_0}|^2 |\eta_{\mathbf{Q}-\mathbf{k}}^{j, m_0}|^2 |J| dv d\mu, \quad (6)$$

which describes the density of states in 3D[25]. For (i), the integration $\int' dv d\mu$ includes all the states. For (ii), the integration $\int' dv d\mu$ excludes the states below the Fermi surfaces. In Eq. (6), μ and ν label the degrees of freedom other than ε , and J denotes the standard Jacobian. These formulas can be also easily adapted to describing the binding of two homo-nuclear fermions where A and B are the same fermionic species.

Equation (5) establishes a direct relation between the interaction U , the density of states $\gamma_{\mathbf{Q}}^\varepsilon$, and $E_{\mathbf{Q}}^{sc}$. Intuition behind it can be gained in the limit of vanishing SOC in case (i), where $E_{th}^{\mathbf{Q}} = \mathbf{Q}^2/(2m_\mu)$ with m_μ the reduced mass of two fermions, and $\gamma_{\mathbf{Q}}^\varepsilon = \gamma_0^\varepsilon = 2\sqrt{2m_\mu\varepsilon}$. Then, $E_{\mathbf{Q}}^{sc}$ is independent of \mathbf{Q} as ensured by Eq. (5), and can be identified as $E_{\mathbf{Q}}^{sc} \equiv \varepsilon_b = -1/(2m_\mu a_s^2)$ [$\hbar \equiv 1$] with $a_s > 0$ the s-wave scattering length, i.e., the binding energy at rest. In this case, Eq. (5) reduces to, in the momentum space representation, the well known renormalization equation for two scattering particles, i.e.,

$$\frac{1}{U} = \frac{m_\mu}{2\pi a_s} - \frac{1}{V} \sum_{\mathbf{k}} \frac{2m_\mu}{\mathbf{k}^2}. \quad (7)$$

Equation (5) thus extends the standard prescription for two interacting fermions to the presence of SOC, where $E_{\mathbf{Q}}^{sc}$ is the counterpart of the binding energy ε_b .

III. ROLE OF INTERACTION

Based on above treatment, below we elucidate how the interaction cooperates with the effect of SOC in deter-

mining the behavior of $E_{\mathbf{Q}}^{sc}$, when the interaction strength a_s^{-1} is tuned in a wide range via Feshbach resonance [22]. To compare to the SOC-free case, we introduce the quantity $\xi_{\mathbf{Q}} \equiv E_{\mathbf{Q}}^{sc} - \varepsilon_b$. For weak SOC that does not significantly alter the density of states, the leading term of $\xi_{\mathbf{Q}}$ can be derived from Eq. (5) as [26]:

$$\xi_{\mathbf{Q}} = - \left[\int_0^\infty \frac{\gamma_{\mathbf{Q}}^\varepsilon}{(\varepsilon - \varepsilon_b)^2} d\varepsilon \right]^{-1} \int_0^\infty \frac{\gamma_{\mathbf{Q}}^\varepsilon - \gamma_0^\varepsilon}{\varepsilon - \varepsilon_b} d\varepsilon. \quad (8)$$

Here we have ignored the modification of the renormalization relation by SOC [27–31]. In discussing the effect of interaction on $\xi_{\mathbf{Q}}$, we will be interested in (i) $\frac{\partial \xi_{\mathbf{Q}}}{\partial a_s^{-1}}$ and (ii) $\Delta_{\mathbf{Q}\mathbf{Q}'} \equiv \xi_{\mathbf{Q}'} - \xi_{\mathbf{Q}}$: The sign of the former reflects how $\xi_{\mathbf{Q}}$ for fixed \mathbf{Q} changes with interaction, while that of the latter tells whether a large or small \mathbf{Q} is energetically favored for a given interaction. Using Eq. (8), we find $\Delta_{\mathbf{Q}\mathbf{Q}'} \simeq - \left[\int_0^\infty \frac{\gamma_{\mathbf{Q}}^\varepsilon}{(\varepsilon - \varepsilon_b)^2} d\varepsilon \right]^{-1} \int_0^\infty \frac{\gamma_{\mathbf{Q}'}^\varepsilon - \gamma_{\mathbf{Q}}^\varepsilon}{\varepsilon - \varepsilon_b} d\varepsilon$. Both of $\xi_{\mathbf{Q}}$ and $\Delta_{\mathbf{Q}\mathbf{Q}'}$ rely crucially on $\gamma_{\mathbf{Q}}^\varepsilon$. Thus, while the form of $\gamma_{\mathbf{Q}}^\varepsilon$ varies with specific setups [see Eq. (6)], its qualitative analysis affords insights into generic behavior of $\xi_{\mathbf{Q}}$, as we elaborate next. In order to give some analyses, we apply the further approximation

$$\begin{aligned} \xi_{\mathbf{Q}} &\simeq - \left[\int_0^\infty \frac{\gamma_0^\varepsilon}{(\varepsilon - \varepsilon_b)^2} d\varepsilon \right]^{-1} \int_0^\infty \frac{\gamma_{\mathbf{Q}}^\varepsilon - \gamma_0^\varepsilon}{\varepsilon - \varepsilon_b} d\varepsilon \\ &\propto \sqrt{-\varepsilon_b} \int_0^\infty \frac{\gamma_{\mathbf{Q}}^\varepsilon - \gamma_0^\varepsilon}{\varepsilon - \varepsilon_b} d\varepsilon. \end{aligned} \quad (9)$$

Consider first the simplest case where $\gamma_{\mathbf{Q}}^\varepsilon - \gamma_0^\varepsilon > 0$ for all energy levels ε [32], i.e., SOC induces an increase in the number of available scattering states at all energies. From Eq. (9), we see $\xi_{\mathbf{Q}} < 0$, hence binding with finite \mathbf{Q} leads to an energy decrease as compared to the SOC-free case, irrespective of the interacting strength. Such energy drop, following from $\frac{\partial \xi_{\mathbf{Q}}}{\partial a_s^{-1}} > 0$, can be further enhanced by increasing a_s^{-1} . If, moreover, $\gamma_{\mathbf{Q}}^\varepsilon$ increases monotonically with \mathbf{Q} , we have $\Delta_{\mathbf{Q}\mathbf{Q}'} < 0$, i.e., $\xi_{\mathbf{Q}}$ decreases with increasing \mathbf{Q} for fixed scattering length. The amplitude of this decrease can be controlled by tuning the scattering length, which enhances with increased a_s^{-1} .

In contrast, if the effect of SOC is such that $\gamma_{\mathbf{Q}}^\varepsilon - \gamma_0^\varepsilon$ alters sign depending on the energy ε of the state, $\xi_{\mathbf{Q}}$ can exhibit a very rich behavior. To demonstrate it, consider $\gamma_{\mathbf{Q}}^\varepsilon - \gamma_0^\varepsilon$ has opposite sign in the low- and high-energy regimes, with a sign flip occurring at the energy ε_0 . Applying the mean value theorem to Eq. (9), we find

$$\int_0^\infty \frac{\gamma_{\mathbf{Q}}^\varepsilon - \gamma_0^\varepsilon}{\varepsilon - \varepsilon_b} d\varepsilon = f_l/(\varepsilon_1 - \varepsilon_b) + f_h/(\varepsilon_2 - \varepsilon_b), \quad (10)$$

with $\varepsilon_1 \in (0, \varepsilon_0)$, and $\varepsilon_2 \in (\varepsilon_0, \infty)$. Here $f_l = \int_0^{\varepsilon_0} (\gamma_{\mathbf{Q}}^\varepsilon - \gamma_0^\varepsilon) d\varepsilon$ and $f_h = \int_{\varepsilon_0}^\infty (\gamma_{\mathbf{Q}}^\varepsilon - \gamma_0^\varepsilon) d\varepsilon$ are the number of scattering states in the low- and high-energy regimes, respectively. Since f_l and f_h have opposite signs, the contribution from the high-energy states to $\xi_{\mathbf{Q}}$ is suppressed by the smaller pre-factor compared to the low-energy states.

Yet, such suppression becomes less significant when a_s^{-1} increases, following similar reasoning as before. We thus expect the sign of $\xi_{\mathbf{Q}}$ to be mainly determined by the low-energy states for large a_s , whereas the high-energy states can become decisive for small a_s . This has interesting physical implications: by tuning the scattering length and hence the sign of $\xi_{\mathbf{Q}}$ and $\Delta_{\mathbf{Q}\mathbf{Q}'}$, we can control whether a bound pair favors nonzero \mathbf{Q} , and even the specific choice of \mathbf{Q} .

IV. TYPICAL BEHAVIORS OF TWO-BODY GROUND STATES

We now show that, combining $E_{th}^{\mathbf{Q}}$, above insights into the cooperative effects of interaction and SOC on $E_{\mathbf{Q}}^{sc}$ allows predictions on generic features of the dispersion $E_{\mathbf{Q}}$. This can be best illustrated in two following cases.

(i) If $E_{th}^{\mathbf{Q}}$ has only one minimum, without interaction, the two-body (molecular) ground state c.m. momentum \mathbf{Q}_g will locate at \mathbf{Q}_1 where $E_{th}^{\mathbf{Q}}$ is minimized. By contrast, adding interaction can strongly modify $E_{\mathbf{Q}}^{sc}$ and thus $E_{\mathbf{Q}}$, according to previous analysis, which renders \mathbf{Q}_g to deviate from \mathbf{Q}_1 . Such deviation intimately depends on the behavior of $E_{\mathbf{Q}}^{sc}$: If $E_{\mathbf{Q}}^{sc}$ varies monotonically with \mathbf{Q} for a fixed scattering length, \mathbf{Q}_g shifts from \mathbf{Q}_1 in such a way that a smaller $E_{\mathbf{Q}}^{sc}$ can be reached. Such shift can be further enhanced by increasing a_s^{-1} , provided it does not qualitatively alter the behavior of $E_{\mathbf{Q}}^{sc}$, i.e., $E_{\mathbf{Q}}^{sc}$ stays increasing (or decreasing) with \mathbf{Q} when varying a_s^{-1} [c.f. inset of Fig. 1(d)]. If, instead, the behavior of $E_{\mathbf{Q}}^{sc}$ undergoes a qualitative change when a_s^{-1} increases, e.g. from increasing to decreasing with \mathbf{Q} [see inset of Fig. 2(c)], \mathbf{Q}_g will first exhibit a zigzag away from \mathbf{Q}_1 before increasing above \mathbf{Q}_1 monotonically [see inset of Fig. 2(d)].

(ii) In general $E_{th}^{\mathbf{Q}}$ can have multiple local minima, each corresponding to a meta-stable state. For individual meta-stable state, the associated c.m. momentum exhibits similar behavior as in (i). An interesting question then concerns how two-body (molecular) ground state transits among multiple meta-stable states when the interaction is tuned. To address it, suppose for simplicity that $E_{th}^{\mathbf{Q}}$ has two degenerate local minima at \mathbf{Q}_1 and \mathbf{Q}_2 respectively, and $E_{\mathbf{Q}}^{sc}$ varies monotonically with \mathbf{Q} for a fixed scattering length. The two-body (molecular) ground state c.m. momentum \mathbf{Q} is expected to be close to \mathbf{Q}_1 or \mathbf{Q}_2 , depending on which corresponds to a smaller $E_{\mathbf{Q}}^{sc}$. If the behavior of $E_{\mathbf{Q}}^{sc}$ can be changed qualitatively by tuning a_s^{-1} , say from increase to decrease with \mathbf{Q} , a transition of the system between the two meta-stable states can be induced. This phenomenon also occurs when the two local minima $E_{th}^{\mathbf{Q}}$ become non-degenerate, due to the competition between $E_{th}^{\mathbf{Q}}$ and $E_{\mathbf{Q}}^{sc}$, which is the origin of the transition discussed in Ref. [16]. In addition, with the increasing of a_s^{-1} , $E_{\mathbf{Q}}^{sc}$ will dominate over $E_{th}^{\mathbf{Q}}$ in

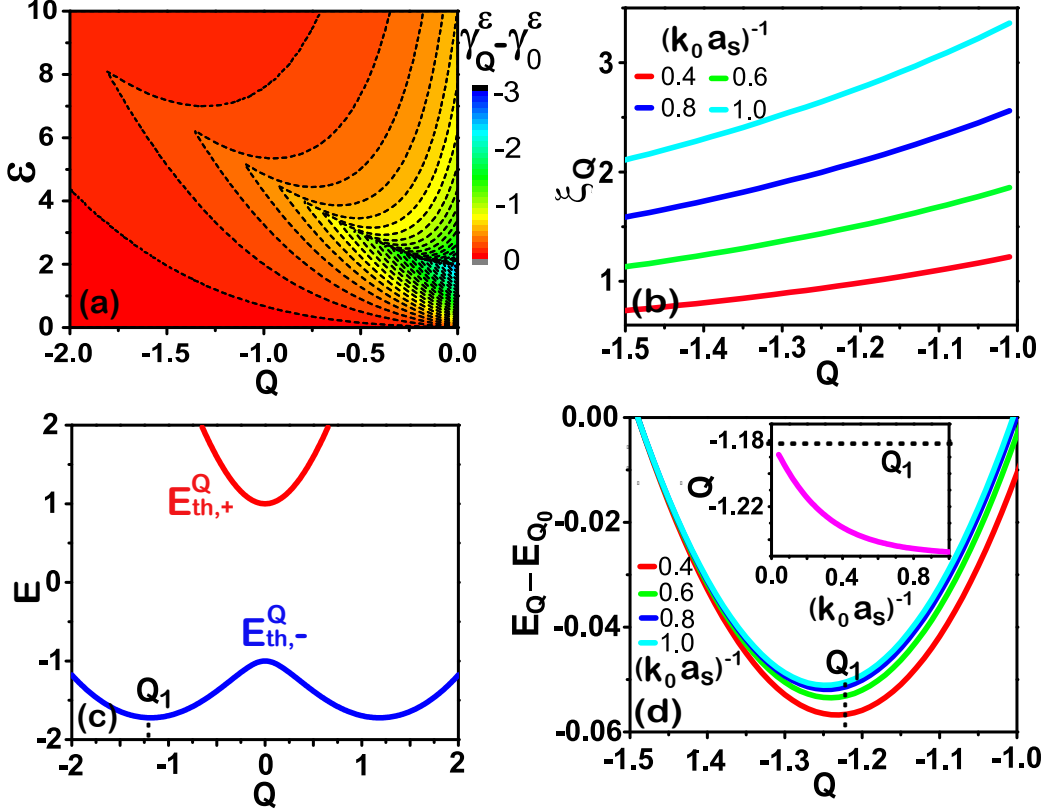


Figure 1. Binding of spin-orbit coupled fermions in the vacuum. (a) The distribution of $\gamma_Q^\varepsilon - \gamma_0^\varepsilon$. (b) ξ_Q as a function of Q with different $(k_0 a_s)^{-1}$ according to Eq.(8). (c) The helicity-dependent threshold energy $E_{th,+}^Q$ ($E_{th,-}^Q$) is the minimum energy of two particles with A in the upper (lower) helicity branch and a c.m. momentum Q . (d) The two-body energy with different interacting strengths by exactly solving Eq. (4). The inset shows the variation of the ground state c.m. momentum. Here $Q_0 = -1.5k_0 e_x$.

determining the dispersion of E_Q . This may qualitative change the dispersion of two-body (molecular) energy, say from a double-well type with two meta-stable states to a single-well type with one meta-stable state, which may cause the disappear of the transition.

V. SPIN-ORBIT COUPLED THREE-COMPONENT FERMI MIXTURE

Previous discussions from Sec. II to Sec. IV are not dependent on the concrete type of the SOC. To give an example, below we present concrete calculations by solving Eq. (4) for a system of interacting Fermi mixture of ^{40}K - ^{40}K - ^6Li (A-A-B), where the atom ^{40}K couples to SOC and the atom ^6Li is spinless. Here, we choose an $(\alpha k_x \sigma_z + h \sigma_x)$ -type SOC which can be readily realized experimentally in ^{40}K [4]. In this three-component mixture, the ^6Li fermions are tuned close to a wide Feshbach resonance with spin up species of ^{40}K [23]. The Hamil-

tonian for the system reads

$$\begin{aligned}
 H = & \sum_{\mathbf{k},\sigma} \varepsilon_{\mathbf{k}}^a a_{\mathbf{k},\sigma}^\dagger a_{\mathbf{k},\sigma} + \sum_{\mathbf{k}} (h a_{\mathbf{k},\uparrow}^\dagger a_{\mathbf{k},\downarrow} + h a_{\mathbf{k},\downarrow}^\dagger a_{\mathbf{k},\uparrow}) \\
 & + \sum_{\mathbf{k}} \varepsilon_{\mathbf{k}}^b b_{\mathbf{k}}^\dagger b_{\mathbf{k}} + \frac{U}{V} \sum_{\mathbf{k},\mathbf{k}',\mathbf{q}} a_{\frac{\mathbf{q}}{2}+\mathbf{k},\uparrow}^\dagger b_{\frac{\mathbf{q}}{2}-\mathbf{k}}^\dagger b_{\frac{\mathbf{q}}{2}-\mathbf{k}'} a_{\frac{\mathbf{q}}{2}+\mathbf{k}',\uparrow} \\
 & + \sum_{\mathbf{k}} (\alpha k_x a_{\mathbf{k},\uparrow}^\dagger a_{\mathbf{k},\uparrow} - \alpha k_x a_{\mathbf{k},\downarrow}^\dagger a_{\mathbf{k},\downarrow}). \quad (11)
 \end{aligned}$$

Here $a_{\mathbf{k},\sigma}$ ($\sigma = \uparrow, \downarrow$) denotes the annihilation operator of a SOC-free particle A with spin σ and momenta \mathbf{k} , while the operator $b_{\mathbf{k}}$ annihilates a particle B with momenta \mathbf{k} . In addition, $\varepsilon_{\mathbf{k}}^{a(b)} = k^2/(2m_{a(b)})$ is the kinetic energy of particle $A(B)$. The SOC parameters h and α are respectively proportional to the Raman coupling strength and the momentum transfer in the Raman process generating the SOC [4]. We also note that via a global pseudo-spin rotation such SOC can be transformed to an equal weight combination of Rashba-type and Dresselhaus-type SOC $(\alpha k_x \sigma_y + h \sigma_z)$ which is the first SOC generated in ultracold atomic gases [2]. Therefore, the $(\alpha k_x \sigma_z + h \sigma_x)$ -type SOC can be interpreted as an equal weight combination

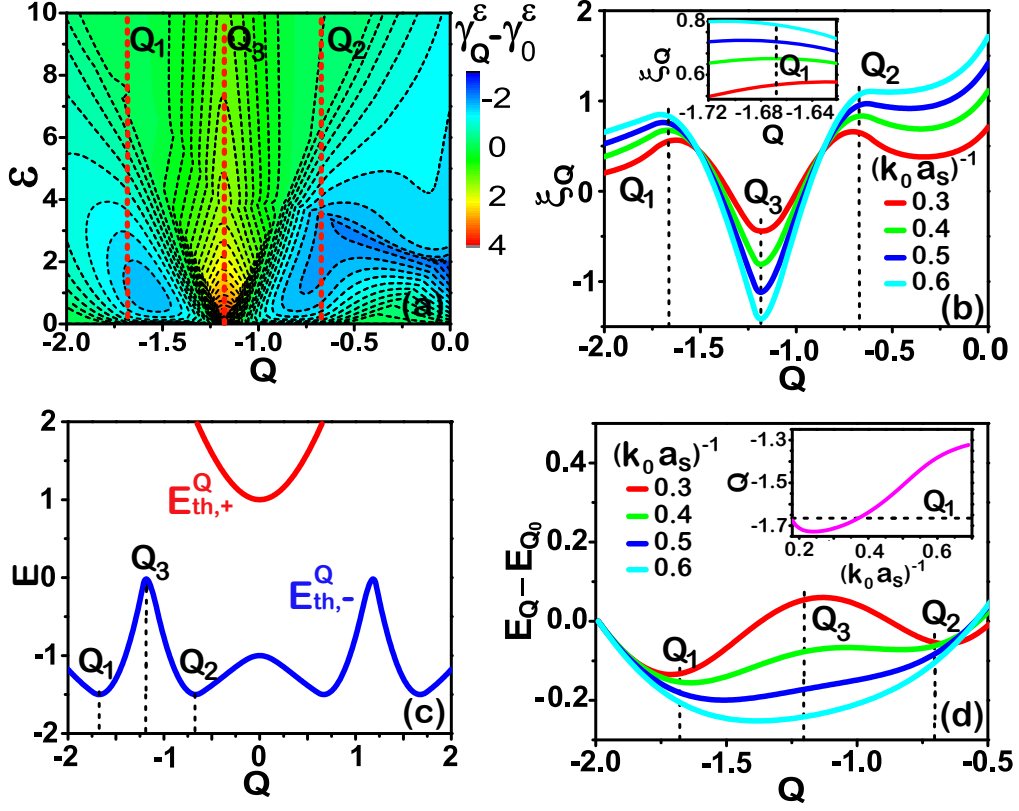


Figure 2. Binding of spin-orbit coupled fermions on top of a Fermi sea in single impurity system. (a) The distribution of $\gamma_Q^\varepsilon - \gamma_0^\varepsilon$. (b) ξ_Q as a function of Q with different $(k_0 a_s)^{-1}$ according to Eq.(8). The inset shows ξ_Q in the region near Q_1 . (c) The threshold $E_{th}^Q = \min\{E_{th,-}^Q, E_{th,+}^Q\}$. The helicity-dependent threshold energy $E_{th,+}^Q$ ($E_{th,-}^Q$) is the minimum energy of two particles with A in the upper (lower) helicity branch and a c.m. momentum Q . (d) The two-body energy with different interacting strengths by exactly solving Eq. (4). The inset shows the variation of the ground state c.m. momentum. Here $Q_0 = -2k_0 e_x$.

of Rashba-type and Dresselhaus-type SOC [4].

In the presence of SOC, the single-particle eigenstates of A in the helicity basis are created by operators $a_{\mathbf{k},\pm}^\dagger = \lambda_{\mathbf{k}}^{\pm,\uparrow} a_{\mathbf{k},\uparrow}^\dagger + \lambda_{\mathbf{k}}^{\pm,\downarrow} a_{\mathbf{k},\downarrow}^\dagger$, with $\lambda_{\mathbf{k}}^{\pm,\uparrow} = \pm \zeta_{\mathbf{k}}^\pm$, $\lambda_{\mathbf{k}}^{\pm,\downarrow} = \zeta_{\mathbf{k}}^\mp$, and $\zeta_{\mathbf{k}}^\pm = [\sqrt{\hbar^2 + \alpha^2 k_x^2} \pm \alpha k_x]^{1/2} / \sqrt{2} [h^2 + \alpha^2 k_x^2]^{1/4}$, with $+$ ($-$) labelling the upper (lower) helicity branch. The single particle dispersions of two helicity branches are $\varepsilon_{\mathbf{k},\pm}^a = \varepsilon_{\mathbf{k}}^a \pm \sqrt{\hbar^2 + \alpha^2 k_x^2}$. Here we have measured the energy in the unit of $E_0 = 2\alpha^2 m_a / \hbar^2$, the momentum in the unit of $k_0 = 2\alpha m_a / \hbar^2$, and $h = 0.4E_0$.

We first present our results for the binding of A and B in the vacuum, as summarized in Fig. 1. The density of states [see Fig. 1(a)] exhibits a monotonic decrease with both Q and ε . As expected, E_Q^{sc} will change monotonically with respect to both Q and a_s^{-1} [see Fig. 1(b)]. Together with E_{th}^Q [see Fig. 1(c)], we see that the actual ground state c.m. momenta will be pulled to the direction with a smaller magnitude than Q_1 and the increase of a_s^{-1} will enhance this tendency [see Fig. 1(d)].

We now turn to the binding of A and B on the top of the Fermi sea of A in the situation where a single impu-

rity of B immerses in a non-interacting Fermi sea of spin-orbit coupled A with the Fermi energy $E_h = -1.5E_0$, as illustrated in Fig. 2. There, both the density of states [see Fig. 2(a)] and E_Q^{sc} [see Fig. 2(b)] exhibit a rich behavior. In addition, from E_{th}^Q in Fig. 2(c), we see that there exist two meta-stable states near Q_1 and Q_2 , respectively. Let us first analyze the c.m. momenta associated with the meta-stable states, e.g., the one formed near Q_1 . Seen from Fig. 2(a), γ_Q^ε for c.m. momentum near Q_1 decreases with Q in the low energy region (e.g. $0 < \varepsilon < 2E_0$), but increases in the high energy region (e.g. $6E_0 < \varepsilon < 10E_0$). In addition, near Q_1 , E_{sc}^Q [see the inset of Fig. 2(b)] shows a qualitative change with increasing of a_s^{-1} . We thus expect from earlier discussions a zigzag behavior of c.m. momenta of the meta-stable state, as confirmed by our results plotted in the inset of Fig. 2(d). Next, we discuss which of the two meta-stable states is energetically favored. Due to the degeneracy of the two local minima of E_{th}^Q , this is determined by the density of states, which is larger near Q_1 than that near Q_2 [see Fig. 2(a)]. Hence the meta-stable state near Q_1

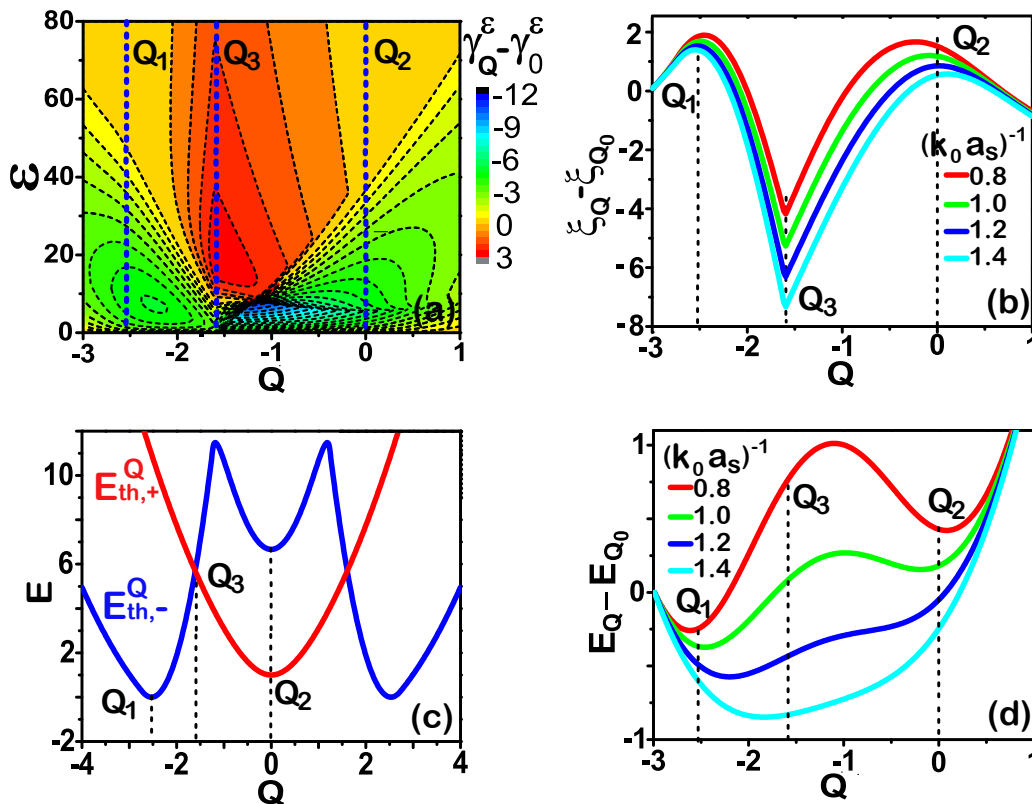


Figure 3. (a) The distribution of $\gamma_Q^\varepsilon - \gamma_0^\varepsilon$. (b) ξ_Q as a function of Q with different $(k_0 a_s)^{-1}$ according to Eq.(8). (c) The threshold energy $E_{th}^Q = \min \{E_{th,-}^Q, E_{th,+}^Q\}$. The helicity-dependent threshold energy $E_{th,+}^Q$ ($E_{th,-}^Q$) is the minimum energy of two particles with A in the upper (lower) helicity branch and a c.m. momentum Q . (d) The two-body energy with different interacting strengths by exactly solving Eq. (4). Here $Q_0 = -3k_0 e_x$.

is energetically favored by E_{sc}^Q [see Fig. 2(b)]. We thus expect the molecular ground state c.m. momentum to be near Q_1 , well agreeing with Fig. 2(d).

Comparing the binding of A and B in the vacuum and on top of the filled Fermi sea, we observe that the presence of Fermi sea not only elevates E_{th}^Q in the regime $Q_1 < Q < Q_2$, giving rise to two minima, but also enhances the density of states there. Consequently, the minimum of E_{sc}^Q occurs at Q_3 , and the two meta-stable states merge together [see Fig. 2(d)] following from previous analysis. We remark that, while the SOC here has dramatically modified the density of states compared to the SOC-free case, our analyses based on perturbation treatment agree remarkably well with the exact numerical results.

VI. CONCLUDING DISCUSSIONS AND SUMMARY

When the Fermi sea has only one Fermi surface, the two meta-stable states formed near Q_1 and Q_2 are favored by the threshold energy and the density of states, respectively, see Fig. 3. In Ref. [16] with high Fermi

energy, tuning the interaction can induce a transition between the two meta-stable states. In contrast, as illustrated in Fig. 3 where the Fermi energy $E_h = 0$, such transition is missing and the increase of a_s^{-1} will eventually cause a merge of the two meta-stable states. With an increase of the Fermi energy, our case crossovers to that discussed in Ref. [16]. In addition, we note that for the single impurity Fermi system we only consider the lowest energy state within our ansatz, the ground state of the system should be given by connecting the molecular ground state to the polaron ground state which describes the particle-hole excitations above the Fermi sea.

Summarizing, we have investigated how the tuning of interacting strength of an attractive s-wave interaction affects two-body energy under certain distribution of the density of states. Combining with the dispersion of the threshold energy, we can predict typical behavior of the two-body bound state when tuning the scattering length and hence the interaction, including the change of the c.m. momentum of the two-body ground state and the competition between multiple meta-stable states. Our perturbation analyses are not dependent on the concrete type of SOC and corroborated by the exact numerical solution of the two-body problem for a spin-orbit coupled

Fermi mixture of ^{40}K - ^{40}K - ^6Li , even though the density of states is significantly altered by the effect of SOC.

VII. ACKNOWLEDGMENTS

We thanks Ying Hu for helpful discussion. The work is supported by the National Basic Research Program of China (973 Program) (Grants No. 2013CBA01502 and No. 2013CB834100), the National Natural Science Foundation of China (Grants No. 11374040, No. 11475027, No. 11575027, and No. 11274051).

-
- [1] Jean Dalibard, Fabrice Gerbier, Gediminas Juzeliūnas, and Patrik Öhberg, *Rev. Mod. Phys.* **83**, 1523 (2011).
- [2] Y.-J. Lin, K. Jimenéz-García, and I. B. Spielman, *Nature (London)* **471**, 83 (2011).
- [3] Jin-Yi Zhang, Si-Cong Ji, Zhu Chen, Long Zhang, Zhi-Dong Du, Bo Yan, Ge-Sheng Pan, Bo Zhao, YouJin Deng, Hui Zhai, Shuai Chen, and Jian-Wei Pan, *Phys. Rev. Lett.* **109**, 115301 (2012).
- [4] Pengjun Wang, Zeng-Qiang Yu, Zhengkun Fu, Jiao Miao, Lianghui Huang, Shijie Chai, Hui Zhai, and Jing Zhang, *Phys. Rev. Lett.* **109**, 095301 (2012).
- [5] Lawrence W. Cheuk, Ariel T. Sommer, Zoran Hadzibabic, Tarik Yefsah, Waseem S. Bakr, and Martin W. Zwierlein, *Phys. Rev. Lett.* **109**, 095302 (2012); Lianghui Huang, Zengming Meng, Pengjun Wang, Peng Peng, Shao-Liang Zhang, Liangchao Chen, Donghao Li, Qi Zhou and Jing Zhang, *Nat. Phys.* **10**, 1038 (2016).
- [6] H. Zhai, *Int. J. Mod. Phys. B* **26**, 1230001 (2012).
- [7] V. Galitski and I. B. Spielman, *Nature*, **494**, 49 (2013).
- [8] H. Zhai, *Rep. Prog. Phys.*, **78**, 026001 (2015).
- [9] Jayantha P. Vyasankere, and Vijay B. Shenoy, *Phys. Rev. B* **83**, 094515 (2011).
- [10] Jayantha P. Vyasankere, Shizhong Zhang, and Vijay B. Shenoy, *Phys. Rev. B* **84**, 014512 (2011).
- [11] Hui Hu, Lei Jiang, Xia-Ji Liu, and Han Pu, *Phys. Rev. Lett.* **107**, 195304 (2011).
- [12] Zeng-Qiang Yu and Hui Zhai, *Phys. Rev. Lett.* **107**, 195305 (2011).
- [13] Ren Zhang, Fan Wu, Jun-Rong Tang, Guang-Can Guo, Wei Yi, and Wei Zhang, *Phys. Rev. A* **87**, 033629 (2013).
- [14] Vijay B. Shenoy, *Phys. Rev. A* **88**, 033609 (2013).
- [15] Fan Wu, Ren Zhang, Tian-Shu Deng, Wei Zhang, Wei Yi, and Guang-Can Guo, *Phys. Rev. A* **89**, 063610 (2014).
- [16] Lihong Zhou, Xiaoling Cui, and Wei Yi, *Phys. Rev. Lett.* **112**, 195301 (2014).
- [17] F. Chevy, *Phys. Rev. A* **74**, 063628 (2006).
- [18] R. Combescot, A. Recati, C. Lobo and F. Chevy, *Phys. Rev. Lett.* **98**, 180402 (2007).
- [19] Sascha Zollner, G. M. Bruun, and C. J. Pethick, *Phys. Rev. A* **83**, 021603(R) (2011).
- [20] Marco Koschorreck, Daniel Pertot, Enrico Vogt, Bernd Frohlich, Michael Feld and Michael Kohl, *Nature* **485**, 619 (2012).
- [21] Wei Yi and Wei Zhang, *Phys. Rev. Lett* **109**, 140402 (2012).
- [22] Cheng Chin, Rudolf Grimm, Paul Julienne, and Eite Tiesinga, *Rev. Mod. Phys.* **82**, 1225 (2010).
- [23] André Schirotzek, Cheng-Hsun Wu, Ariel Sommer, and Martin W. Zwierlein, *Phys. Rev. Lett.* **102**, 230402 (2009); M. Koschorreck, D. Pertot, E. Vogt, B. Fröhlich, M. Feld, and M. Köhl, *Nature (London)* **485**, 619 (2012).
- [24] W. Ketterle and M. W. Zwierlein, *Rivista del Nuovo Cimento* **31**, 247-422 (2008).
- [25] We note that for homo-nuclear systems, our derivation for $\gamma_{\mathbf{Q}}^{\epsilon}$ reduces to the singlet density of states as discussed in Ref. [14].
- [26] With Eq.(5) and renormalization equation, we have $\int_0^{\infty} \frac{\gamma_0^{\epsilon}}{\epsilon_b - \epsilon} d\epsilon = \int_0^{\infty} \frac{\gamma_{\mathbf{Q}}^{\epsilon}}{\xi_{\mathbf{Q}} + \epsilon_b - \epsilon} d\epsilon$. The right hand of the equation can be written as follow $\int_0^{\infty} \frac{\gamma_{\mathbf{Q}}^{\epsilon}}{\xi_{\mathbf{Q}} + \epsilon_b - \epsilon} d\epsilon = \int_0^{\infty} [\frac{\gamma_{\mathbf{Q}}^{\epsilon}}{\epsilon_b - \epsilon} - \frac{\xi_{\mathbf{Q}} \gamma_{\mathbf{Q}}^{\epsilon}}{(\epsilon_b - \epsilon)^2} + \frac{\xi_{\mathbf{Q}}^2 \gamma_{\mathbf{Q}}^{\epsilon}}{(\epsilon_b - \epsilon)^3} + \dots] d\epsilon$. To first order of $\xi_{\mathbf{Q}}$ ($|\frac{\xi_{\mathbf{Q}}}{\epsilon_b}| \ll 1$), we arrive Eq.(8).
- [27] Xiaoling Cui, *Phys. Rev. A* **85**, 022705 (2012).
- [28] Peng Zhang, Long Zhang, and Wei Zhang, *Phys. Rev. A* **86**, 042707 (2012).
- [29] Peng Zhang, Long Zhang, and Youjin Deng, *Phys. Rev. A* **86**, 053608 (2012).
- [30] Yuxiao Wu and Zhenhua Yu, *Phys. Rev. A*, **87**, 032703 (2013).
- [31] Hao Duan, Li You, and Bo Gao, *Phys. Rev. A*, **87**, 052708 (2013).
- [32] the analysis for the case with $\gamma_{\mathbf{Q}}^{\epsilon} - \gamma_0^{\epsilon} > 0$ is similar.